Coordination Chemistry

Deutsche Ausgabe: DOI: 10.1002/ange.201601678
Internationale Ausgabe: DOI: 10.1002/anie.201601678

Ultrafine Metal–Organic Right Square Prism Shaped Nanowires

Ken-ichi Otake, Kazuya Otsubo, Kunihisa Sugimoto, Akihiko Fujiwara, and Hiroshi Kitagawa**

Abstract: *We report the structural design and control of electronic states of a new series of ultrafine metal–organic right square prism-shaped nanowires. These nanowires have a very small inner diameter of about 2.0 Å, which is larger than hydrogen and similar to xenon atomic diameters. The electronic states of nanowires can be widely controlled by substitution of structural components. Moreover, the platinum homometallic nanowire shows a 100 times higher proton conductivity than a palladium/platinum heterometallic one depending on the electronic states.*

Semiconducting one-dimensional (1D) nanowires have long been studied for a variety of future nanoelectronic applications including transistors, supercapacitors, photovoltaics, sensors, and memories.[1] Nanowires are also important for studying low-dimensional physics such as spin-density waves, charge-density waves, solitons, polarons, large optical nonlinearity and Tomonaga–Luttinger liquid behavior.[2] Various materials such as organic, single/multi-elements, metal-oxide and chalcogenide nanowires have been extensively explored.[3] Nanowires based on coordination bonds have attracted particular interest recently because their structure can easily be modified.[4] Compared with other nanowires, coordination nanowires have several advantages of systematic control of chemical and physical properties, including electrical conductivity and magnetic properties through substitution of structural components such as metal ions and organic ligands.

[*] K.-i. Otake, Dr. K. Otsubo, Prof. H. Kitagawa
Division of Chemistry, Graduate School of Science
Kyoto University, Sakyo-ku, Kyoto 606-8502 (Japan)
E-mail: kazuya@kuchem.kyoto-u.ac.jp
kitagawa@kuchem.kyoto-u.ac.jp
Dr. K. Sugimoto
Japan Synchrotron Radiation Research Institute (JASRI)
SPring-8, Sayo-cho, Sayo-gun, Hyogo 679-5198 (Japan)
Prof. A. Fujiwara
Department of Nanotechnology for Sustainable Energy
Graduate School of Science and Technology
Kwansei Gakuin University, Sanda, Hyogo 669-1337 (Japan)
Prof. H. Kitagawa
INAMORI Frontier Research Center, Kyushu University
Motooka 744, Nishi-ku, Fukuoka 819-0395 (Japan)
Prof. H. Kitagawa
Institute for Integrated Cell-Material Sciences (iCeMS)
Kyoto University, Yoshida, Sakyo-ku, Kyoto 606-8501 (Japan)

Supporting information for this article, including details of the synthetic methods, X-ray crystallographic information, IR spectroscopy, SEM-EDX spectroscopy, XPS spectroscopy, Raman spectroscopy, single-crystal impedance spectroscopy, and discussion about the electronic states, can be found under: http://dx.doi.org/10.1002/anie.201601678.

Among the coordination nanowires, 1D halogen-bridged transition-metal complexes (MX-chains) are known as metal complex nanowires with 1D electronic systems.[5] Recently, we have investigated the electronic properties of multi-strand nanowire compounds[6] using MX-chains with organic linkers. The electronic properties of such nanowire systems, such as valence arrangements and optical band gap, depend strongly on the number of constituent wires.[6d,e]

Here, we report syntheses and electronic properties of a new series of ultrafine metal–organic right square prism-shaped nanowires with very small inner-diameters of about 2.0 Å. A platinum homometallic nanowire assembly was synthesized using oxidative polymerization of a square platinum complex. By using coordination-driven self-assembly, three kinds of isostructural palladium/platinum heterometallic nanowires were also obtained. In addition, we demonstrated that the optical band gap can be widely controlled between 2 and 4 eV by substitution of structural components. Moreover, the proton conductivity of the platinum homometallic nanowire was 100 times higher than that of a heterometallic one.

In this study, we have focused on the cyano-bridged square metal complex unit **1** as a building block of an ultrafine right square prism-shaped nanowire. This complex is constructed from the self-assembly of *cis*-capped metal cyanide and metal nitrate complexes (Figure 1 a), then the target square prism-shaped nanowire is constructed through oxidative polymerization of **1** (Figure 1 b). By using the same strategy, heterometallic nanowires can be also formed from the heterometallic square unit **2** (Figure 1 a,c). The coordination-driven self-assembly reaction of two appropriate mononuclear complexes offers isostructural heterometallic square prism-shaped nanowire (Figure 1 d and Figure S1 in the Supporting Information).[7]

Oxidative polymerization of a square divalent complex $[Pt(dach)(CN)]_4(NO_3)_4$ (**1**) using Br_2 offered a novel homometallic right square prism-shaped Pt complex $[Pt(dach)(CN)Br]_4(NO_3)_4$ (**3**) (Figures S2 a and S3). Single-crystal X-ray diffraction (SCXRD) analysis revealed that cyano-bridged metal squares with a very short Pt–Pt distance of approximately 5.1 Å are connected by bridging-bromide ions to form the ultrafine right square prism-shaped nanowire structure shown in Figure 2 a–c.

The compact CN^- connector results in a tightly-packed quadruple-stranded structure consisting of four MX-chains with an inner-diameter of about 2.0 Å (Figure 2 b). This size is larger than hydrogen and similar to xenon atomic diameters. The bridging bromide ions are disordered with half of the occupancies around the midpoint between adjacent Pt sites, indicating that the electronic state within one constituent MX-chain of **3** corresponds to the mixed-valence state ($\cdots Pt^{II}\cdots X\text{-}Pt^{IV}\text{-}X\cdots$).[5] Overall, the nanowire has a net 4+

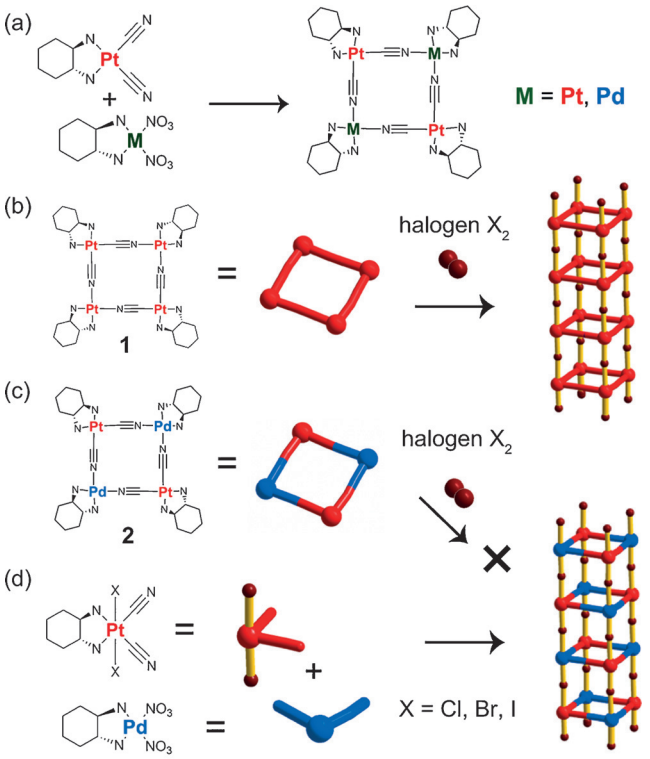

Figure 1. Schematic representation of the bottom-up synthesis of a square unit and right square prism-shaped nanowires. a) Self-assembly of a square complex unit. b) Oxidative polymerization of homometallic square complex (**1**). c) Oxidative polymerization of heterometallic square complex (**2**). d) Facile synthetic strategy of heterometallic right square nanowires.

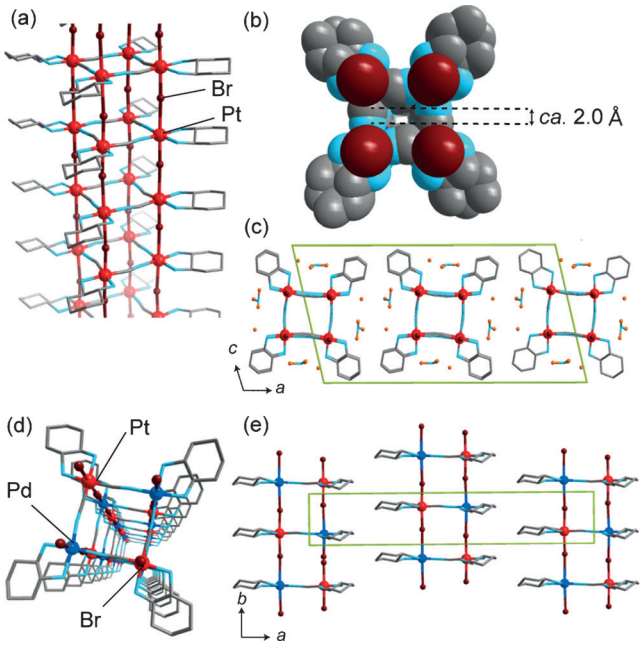

Figure 2. Crystal structures of **3** and **5** at 100 K. One of the disordered components is shown for clarity. a) Pt homometallic right square nanowire structure of **3**. b) Space-filling model of **3**. c) Perspective view of 3D packing of **3** in the *ac* plane. d) Pd/Pt heterometallic right square-shaped nanowire structure of **5**. e) Perspective view of 3D packing of **5** in the *ab* plane. Red, blue, and brown spheres represent Pt, Pd, and Br, respectively. In (c) counteranions (NO_3^-) and crystallization water molecules are also shown.

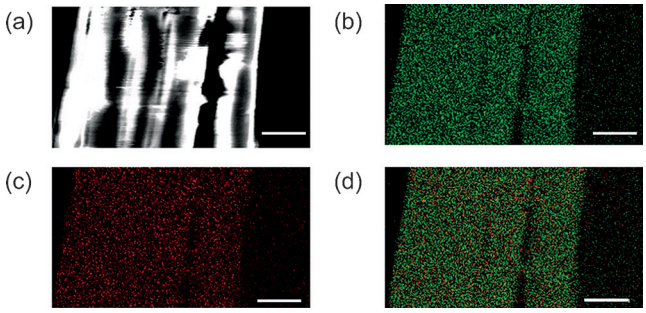

Figure 3. a) Dark-field SEM image of single crystals of **5**. b) Pd and c) Pt L-shell SEM-EDX maps. d) Overlay image of the EDX maps shown in b) and c). The scale bars correspond to 10 μm. (red, Pd; green, Pt).

charge per $[Pt(dach)(CN)Br]_4$ unit; this charge is balanced by nitrate anions that reside between the nanowires along the *b* direction. The nearest Pt distance between each nanowire is 10.5 Å, which is more than twice the intrawire Pt–Pt distance (5.1 Å), suggesting that each nanowire is well-isolated in the crystalline state.

Next, we attempted syntheses of heterometallic right square nanowires via the oxidative polymerization of a heterometallic square unit **2**, as shown in Figure 1c. However, these approaches were not successful. On the other hand, by using the coordination-driven self-assembly reaction of $Pt(dach)(CN)_2X_2$ and $Pd(dach)(NO_3)_2$ (dach = (1R,2R)-(−)-diaminocychlohexane; X = Cl, Br, I) (Figure 1d, S2b–d and S3), we successfully synthesized three heterometallic counterparts of **3**, $[Pd(dach)]_2[Pt(dach)(CN)_2X_2]_2(NO_3)_4$ (**4** (X = Cl), **5** (X = Br), **6** (X = I)). The results of elemental analyses and scanning electron microscopy/energy dispersive X-ray spectroscopy (SEM/EDX) measurements indicated that the Pd and Pt ions spread homogeneously throughout the crystals with the composition ratio of Pd:Pt = 1:1 in **4**–**6** (Figures 3 and S4–S7). SCXRD studies revealed that the crystal structures of **4**, **5**, and **6** are isostructural with **3** (Figure 2c,d for **5**, and Table S1). In addition, the site occupancy factors of all metal sites were determined to be Pd 0.5 and Pt 0.5, respectively. This is because the *ac*-plane orientation of each right square prism-shaped nanowire would be random in the crystal, and the averaged structure was observed in X-ray studies (Figure S8). In fact, the observed lattice constants along the nanowire direction (*b** direction) are half the expected Pt-X-Pd-X-Pt lengths. X-ray photoelectron spectroscopy (XPS) measurements were performed to confirm the valence state of **3**–**6** (Figure S9–10). Pt 4f core-level spectra of **3** indicated mixed valence of Pt^{II} and Pt^{IV} (Figure S9a), which is consistent with the result of the structural analysis. For **5**, the binding energies of Pt 4f and Pd 3d leveles are similar to those of the heterometallic MX-chain,[8] indicating that the valence states of Pd and Pt in **5** are Pd^{II} and Pt^{IV}, respectively (Figure S9b,c). The same results were obtained for **4** and **6** (Figure S10; the XPS data of **3**–**6** are summarized in Table S2). The observed X-ray diffuse scatterings with finite

linewidth at $k \pm 1/2$ (leg direction) indicated twofold periodicity of Pd^{II} and Pt^{IV} (···Pd^{II}···X-Pt^{IV}-X···; Figure S11). These results indicated that the heterometallic right-square-shaped nanowires **4**–**6** are composed of Pd^{II} and Pt^{IV} in an ordered arrangement within one nanowire, as expected from the synthesis method (Figure 1c).

To obtain further information about the electronic states, Raman and diffuse reflectance spectra were collected. The intense peaks of symmetrical stretching modes ν(Pt-X) (X = Cl, Br, I) with overtones were clearly observed at 191 (**3**), 326 (**4**), 198 (**5**), and 132 cm^{-1} (**6**) in Raman spectra (Figure S12). With decreasing temperatures, the overtone progressions became clearer for homometallic nanowire compared with those of heterometallic one (Figure S13). Because such resonance Raman peaks of ν(Pt-X) are forbidden in the avererage valence state, the results indicated that the nanowires are in the mixed-valence state (···M^{II}···X-Pt^{IV}-X···; M = Pt (**3**), Pd (**4**–**6**))[8] from low temperature to room temperature. In diffuse reflectance spectra, intense and broad bands were observed at about 2.5 eV (**3**), 4.0 eV (**4**), 3.0 eV (**5**), and 2.2 eV (**6**), respectively (Figure 4). These bands are assignable

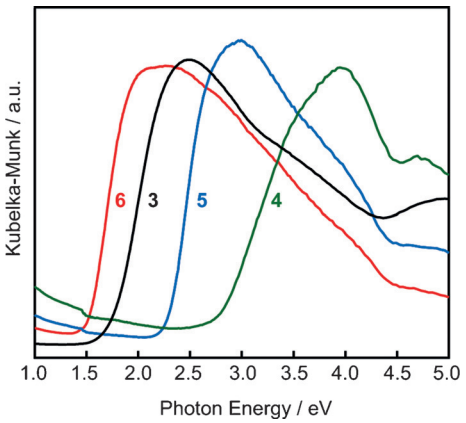

Figure 4. Diffuse reflectance spectra of **3**, **4**, **5**, and **6** at room temperature.

to the inter-valence charge-transfer (IVCT) transitions from the M^{II} to the adjacent Pt^{IV} (M = Pt for **3**, and M = Pd for **4**–**6**). These results clearly demonstrate that their electronic states are the mixed-valence state and correspond to the class II mixed-valence compounds of the Robin–Day classification.[9] As is clearly observed, with the change in bridging halide, the IVCT band gaps increased in the order of I < Br < Cl, indicating that the optical band gap can be wildly controlled. The IVCT band gap in **5** is larger than that of **3**. This is because of the difference in energy levels between Pd^{II} 4d and Pt^{II} 5d and the small overlap integral in **5**,[8] which is supported by the observed higher binding energies of Pt^{IV} in XPS spectra and higher frequency ν(Pt-Br) mode in **5**. Previous studies of MX compounds have shown that there is a linear relationship between IVCT band gap and the degree of distortion of bridging halide ion.[10] In addition, it was found that the linear correlation of two-legged MX-ladder nanowires have a larger slope than that of MX-chain systems.[6e] In the present case, they also show a similar linear relationship, but with a larger slope (Figure S14). The larger IVCT band gaps compared with those of other existing systems indicate that ultrafine right square prism-shaped nanowire systems have different electronic states with other MX-systems (Figure S15 and S16).[11]

Because the 1D hydrogen-bond networks composed of NO_3^-, H_2O and the -NH_2 of dach ligand are formed in the crystal (Figure 2c and S17), we expected the proton conduction[12] of the nanowires. Therefore, impedance measurements were performed using single crystals of **3** and **5** along the wire directions (*b* direction; Figure S18 insets). We also confirmed that their dc conductivities are less than the lower limit of measurement, indicating that the contribution of electron conduction of the nanowires could be ruled out. On the other hand, when measured with impedance at relative humidity of 95%, **3** and **5** gave semi-circle responses in the Nyquist plots that varied with temperature (Figure S18). At 35 °C, their proton conductivities reached 1.29×10^{-5} S cm^{-1} for **3** and 1.54×10^{-7} S cm^{-1} for **5**. As clearly seen, **3** shows 100 times higher proton conductivity than that of **5**. From the Arrhenius plots of the proton conductivity, the activation energies were estimated to be 0.54 for **3** and 0.43 eV for **5**, respectively (Figure 5). Therefore, the mechanism of proton conduction of **3** and **5** is expected to be Grotthus type.[12a] Considering that **3** and **5** are isostructural, the lower optical gap (i.e. lower charge modulation) might result in higher proton conductivity.

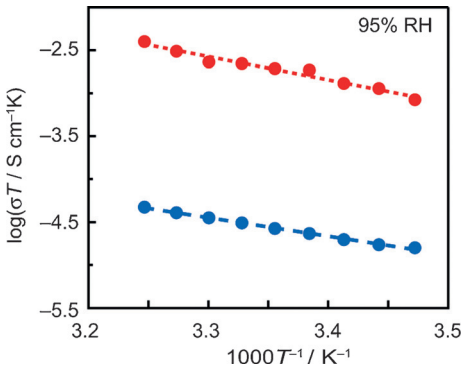

Figure 5. Temperature dependence of the proton conductivity of single crystals of **3** and **5** at a relative humidity of 95%. Red and blue circles denote the data for **3** and **5**, respectively.

In summary, we have successfully synthesized a series of ultrafine metal–organic right square prism-shaped nanowires with a very small inner-diameter of about 2.0 Å. The homometallic platinum mixed-valence nanowire assembly was synthesized using oxidative polymerization of cyano-bridged platinum complex using elemental bromine. In addition, three isostructural palladium/platinum heterometallic nanowires were also obtained via coordination-driven self-assembly. The electronic state of these nanowires can be controlled via substitution of structural components. Moreover, we demonstrated the homometallic nanowire shows 100 times higher proton conductivity than that of heterometallic one. Our results will provide a valuable insight into the

realization of attractive physical properties in hollow nanowire materials. Our ongoing work is focused on systematic control of the electronic properties of multistranded nanowires via carrier doping and the introduction of magnetic ions.

Acknowledgements

This work was supported by Core Research for Evolutional Science and Technology (CREST) from the Japan Science and Technology Agency (JST), Grants-in-Aid for Scientific Research (A) (grant numbers 20350030 and 23245012) and Grant-in-Aid for Young Scientists (A) (grant number 15H05479) from the Japan Society for the Promotion of Science (JSPS). Synchrotron XRD measurements were supported by the Japan Synchrotron Radiation Research Institute (JASRI; proposal numbers 2011B4907, 2012B1558, 2012B4912, 2013A1480, 2013B1400, 2014A1406, and 2014B1440).

Keywords: charge transfer · heterometallic complexes · nanostructures · proton conduction · self-assembly

How to cite: *Angew. Chem. Int. Ed.* **2016**, *55*, 6448–6451
Angew. Chem. **2016**, *128*, 6558–6561

[1] a) W. Lu, C. M. Leiber, *Nat. Mater.* **2007**, *6*, 841–850; b) A. I. Hochbaum, P. Yang, *Chem. Rev.* **2010**, *110*, 527–546; c) A. Koka, H. A. Sadano, *Nat. Commun.* **2013**, *4*, 2682; d) T. Ernst, *Science* **2013**, *340*, 1414–1415; e) L. Mai, X. Tian, X. Xu, L. Chang, L. Xu, *Chem. Rev.* **2014**, *114*, 11828–11862; f) C. Busche, L. Vilà-Nadal, J. Yan, H. N. Miras, D.-L. Long, V. P. Georgiev, A. Asenov, R. H. Pedersen, N. Gadegaard, M. M. Mirza, D. J. Paul, J. M. Poblet, L. Cronin, *Nature* **2014**, *515*, 545–549.

[2] a) A. O. Patil, A. J. Heeger, F. Wudl, *Chem. Rev.* **1988**, *88*, 183–200; b) H. Kishida, H. Matsuzaki, H. Okamoto, T. Manabe, M. Yamashita, Y. Taguchi, Y. Tokura, *Nature* **2000**, *405*, 929–932; c) H. Ishii, H. Kataura, H. Shiozawa, H. Yoshioka, H. Otsubo, Y. Takayama, T. Miyahara, S. Suzuki, Y. Achiba, M. Nakatake, T. Narimura, M. Higashiguchi, K. Shimada, H. Namatame, M. Taniguchi, *Nature* **2003**, *426*, 540–544; d) K. Otsubo, A. Kobayashi, H. Kitagawa, M. Hedo, Y. Uwatoko, H. Sagayama, Y. Wakabayashi, H. Sawa, *J. Am. Chem. Soc.* **2006**, *128*, 8140–8141.

[3] a) C. N. R. Rao, F. L. Deepak, G. Gundiah, A. Govindaraj, *Prog. Solid State Chem.* **2003**, *31*, 5–147; b) A. L. Briseno, S. C. B. Mannsfeld, S. A. Jenekhe, Z. Bao, Y. Xia, *Mater. Today* **2008**, *11*, 38–47; c) D. Mihailovic, *Prog. Mater. Sci.* **2009**, *54*, 309–350; d) E. M. Freer, O. Grachev, X. Duan, S. Martin, D. Stumbo, *Nat. Nanotechnol.* **2010**, *5*, 525–530; e) S.-Y. Min, T.-S. Kim, Y. Lee, H. Cho, W. Xu, T.-W. Lee, *Small* **2015**, *11*, 45–62; f) Z. Zhang, T. Murayama, M. Sadakane, H. Ariga, N. Yasuda, N. Sakaguchi, K. Asakura, W. Ueda, *Nat. Commun.* **2015**, *6*, 7731.

[4] a) N. Tuccitto, V. Feffi, M. Cavazzini, S. Quici, G. Zhavnerko, A. Licciardello, M. A. Rampi, *Nat. Mater.* **2009**, *8*, 41–46; b) R. Mas-Ballesté, J. Gómez-Herrero, F. Zamora, *Chem. Soc. Rev.* **2010**, *39*, 4220–4233; c) C. Hermosa, J. V. Alvarez, M.-A. Azani, C. J. Gómez-Garcia, M. Fritz, J. M. Soler, J. Gómez-Herrero, C. Gómez-Navarro, F. Zamora, *Nat. Commun.* **2013**, *4*, 1709; d) X. Yin, S. A. Warren, Y.-A. Pan, K.-C. Tsao, D. L. Gray, J. Bertke, H. Yang, *Angew. Chem. Int. Ed.* **2014**, *53*, 14087–14091; *Angew. Chem.* **2014**, *126*, 14311–14315; e) H. M. Yamamoto, *CrystEngComm* **2014**, *16*, 2857–2868; f) R. Sakamoto, K.-H. Wu, R. Matsuoka, H. Maeda, H. Nishihara, *Chem. Soc. Rev.* **2015**, *44*, 7698–7714.

[5] a) S. Kida, *Bull. Chem. Soc. Jpn.* **1965**, *38*, 1804; b) L. V. Interrante, K. W. Browall, F. P. Bund, *Inorg. Chem.* **1974**, *13*, 1158–1162; c) H. Okamoto, M. Yamashita, *Phys. Rev. Lett.* **1992**, *69*, 2248; d) S. Takaishi, H. Miyasaka, K. Sugiura, M. Yamashita, H. Matsuzaki, H. Kishida, T. Takami, *Angew. Chem. Int. Ed.* **2004**, *43*, 3171–3175; *Angew. Chem.* **2004**, *116*, 3233–3237; e) S. Takaishi, M. Takamura, T. Kajiwara, H. Miyasaka, *J. Am. Chem. Soc.* **2008**, *130*, 12080–12084; f) H. Iguchi, S. Takaishi, D. Jiang, J. Xie, M. Yamashita, A. Uchida, H. Kawaji, *Inorg. Chem.* **2013**, *52*, 13812–13814.

[6] a) A. Kobayashi, H. Kitagawa, *J. Am. Chem. Soc.* **2006**, *128*, 12066–12067; b) K. Otsubo, Y. Wakabayashi, J. Ohara, S. Yamamoto, H. Matsuzaki, H. Okamoto, H. Kitagawa, *Nat. Mater.* **2011**, *10*, 291–295; c) T. Yamada, K. Otsubo, R. Makiura, H. Kitagawa, *Chem. Soc. Rev.* **2013**, *42*, 6655–6669; d) K. Otsubo, A. Kobayashi, K. Sugimoto, A. Fujiwara, H. Kitagawa, *Inorg. Chem.* **2014**, *53*, 1229–1240; e) K. Otsubo, H. Kitagawa, *CrystEngComm* **2014**, *16*, 6277–6286.

[7] a) M. Fujita, M. Tominaga, A. Hori, B. Therrien, *Acc. Chem. Res.* **2005**, *38*, 369–378; b) C. G. Oliveri, P. A. Ulmann, M. J. Wiester, C. A. Mirkin, *Acc. Chem. Res.* **2008**, *41*, 1618–1629; c) R. Chakrabarty, P. S. Mukherjee, P. J. Stang, *Chem. Rev.* **2011**, *111*, 6810–6918; d) T. R. Cook, Y.-R. Zheng, P. J. Stang, *Chem. Rev.* **2013**, *113*, 734–777; e) L. Xu, Y, -X. Wang, L, -J. Chen, H, -B. Yang, *Chem. Soc. Rev.* **2015**, *44*, 2148–2167; f) S.-L. Huang, Y.-J. Lin, Z.-H. Li, G.-X. Jin, *Angew. Chem. Int. Ed.* **2014**, *53*, 11218–11222; *Angew. Chem.* **2014**, *126*, 11400–11404; g) C. Klein, C. Gütz, M. Bogner, F. Topić, K. Rissanen, A. Lützen, *Angew. Chem. Int. Ed.* **2014**, *53*, 3739–3742; *Angew. Chem.* **2014**, *126*, 3814–3817.

[8] a) G. C. Papavassiliou, D. Layek, *Z. Naturforsch. B* **1982**, *37*, 1406; b) N. Matsumoto, M. Yamashita, S. Kida, *Bull. Chem. Soc. Jpn.* **1978**, *51*, 2334; c) K. Toriumi, M. Yamashita, I. Murase, *Chem. Lett.* **1986**, 1753; d) Y. Wada, T. Mitani, K. Toriumi, M. Yamashita, *J. Phys. Soc. Jpn.* **1989**, *58*, 3013.

[9] M. B. Robin, P. Day, *Adv. Inorg. Chem. Radiochem.* **1967**, *9*, 247–422.

[10] a) Y. Wada, T. Mitani, M. Yamashita, T, Koda, *J. Phys. Soc. Jpn.* **1985**, *54*, 3143; b) H. Okamoto, T. Mitani, K. Toriumi, M. Yamashita, *Mater. Sci. Eng. B* **1992**, *13*, L9–14; c) B. Scott, S. P. Love, G. S. Kanner, S. R. Johnson, M. P. Wilkerson, M. Berkey, B. I. Swanson, A. Saxena, X. Z. Huang, A. R. Bishop, *J. Mol. Struct.* **1995**, *356*, 207–229.

[11] a) S. Yamamoto, J. Ohara, *Phys. Rev. B* **2007**, *76*, 235116; b) K. Iwano, Y. Shimoi, *J. Phys. Soc. Jpn.* **2007**, *76*, 063708; c) J. Ohara, S. Yamamoto, *EPL* **2009**, *87*, 17006.

[12] a) N. Agmon, *Chem. Phys. Lett.* **1995**, *244*, 456–462; b) K.-D. Kreuer, S. J. Paddison, E, Spohr, M. Schuster, *Chem. Rev.* **2004**, *104*, 4637–4678; c) M. Sadakiyo, T. Yamada, H. Kitagawa, *J. Am. Chem. Soc.* **2009**, *131*, 9906–9907; d) M. Yoon, K. Suh, S. Natarajan, K. Kim, *Angew. Chem. Int. Ed.* **2013**, *52*, 2688–2700; *Angew. Chem.* **2013**, *125*, 2752–2764.

Received: February 17, 2016
Revised: March 9, 2016
Published online: April 15, 2016

